



**HAL**  
open science

## A challenge for x-ray photoelectron spectroscopy characterization of Cu(In,Ga)Se<sub>2</sub> absorbers: The accurate quantification of Ga/(Ga + In) ratio

Solène Béchu, Anais Loubat, Muriel Bouttemy, Jackie Vigneron, Jean-Louis  
Gentner, Arnaud Etcheberry

### ► To cite this version:

Solène Béchu, Anais Loubat, Muriel Bouttemy, Jackie Vigneron, Jean-Louis Gentner, et al..  
A challenge for x-ray photoelectron spectroscopy characterization of Cu(In,Ga)Se<sub>2</sub> absorbers:  
The accurate quantification of Ga/(Ga + In) ratio. *Thin Solid Films*, 2019, 669, pp.425-429.  
10.1016/j.tsf.2018.11.029 . hal-03116822

**HAL Id: hal-03116822**

**<https://hal.science/hal-03116822>**

Submitted on 20 Jan 2021

**HAL** is a multi-disciplinary open access archive for the deposit and dissemination of scientific research documents, whether they are published or not. The documents may come from teaching and research institutions in France or abroad, or from public or private research centers.

L'archive ouverte pluridisciplinaire **HAL**, est destinée au dépôt et à la diffusion de documents scientifiques de niveau recherche, publiés ou non, émanant des établissements d'enseignement et de recherche français ou étrangers, des laboratoires publics ou privés.

1           **A challenge for X-Ray Photoelectron Spectroscopy characterization of**  
2           **Cu(In,Ga)Se<sub>2</sub> absorbers: the accurate quantification of Ga / (Ga + In) ratio**

3 Solène Béchu<sup>1,2</sup>, Anais Loubat<sup>1,2</sup>, Muriel Bouttemy<sup>1,2</sup>, Jackie Vigneron<sup>1,2</sup>, Jean-Louis Gentner<sup>3</sup>, Arnaud  
4 Etcheberry<sup>1,2\*</sup>

5  
6 <sup>1</sup> Institut Photovoltaïque d'Ile-de-France (IPVF), 30 RD 128, 91120 Palaiseau, France.

7 <sup>2</sup> Institut Lavoisier de Versailles (ILV), Université Paris-Saclay, CNRS-UVSQ, 45 av. des Etats-Unis,  
8 Versailles, 78035, France.

9 <sup>3</sup> Almae Technologies SAS, Route de Nozay, 91460 Marcoussis, France

10 \* Corresponding author: [arnaud.etcheberry@uvsq.fr](mailto:arnaud.etcheberry@uvsq.fr)

11 **Abstract**

12 CIGS (Cu(In,Ga)Se<sub>2</sub>) layers are among the more efficient photovoltaic absorbers for thin film solar  
13 cells and remain competitive in the worldwide landscape of solar cells devices and modules with also  
14 new emerging markets (flexible or metallic substrates, tandem, low or high band gap CIGS...). Their  
15 properties are governed by different key composition parameters, and among them the GGI ratio  
16 ( $[\text{Ga}]/([\text{Ga}]+[\text{In}])$ ) which controls the gap value. Indeed, the GGI determination is an important  
17 metrological challenge at the surface of the CIGS layer, particularly before the buffer deposition.  
18 Using X-Ray Photoelectron Spectroscopy (XPS), we propose here a specific methodology to  
19 determine this ratio at the surface. In order to, a surface preparation of the CIGS by chemical  
20 treatments, combining an initial flattening by HBr:Br<sub>2</sub>:H<sub>2</sub>O etching with a finishing step performed in  
21 KCN:H<sub>2</sub>O, is implemented. This chemical engineering leads to a quasi "perfect" surface, flattened and  
22 cleared from surface oxide and selenide phase on which our XPS methodology for GGI determination  
23 is tested. The photopeaks choice to obtain the most coherent GGI ratio quantification is discussed. In

24 particular we focus on the Ga3d-In4d region, situated in narrow binding energy domain, and discuss  
25 why this photopeak combination can be considered as the most adapted for a representative GGI  
26 determination. Quantitative fitting procedure of the Ga3d-In4d region is qualified on a reference  
27 epitaxial  $\text{In}_x\text{Ga}_{1-x}\text{As}$  layer and its implementation in the CIGS case is shown.

## 28 **Keywords**

29 copper indium gallium selenide; X-ray photoelectron spectroscopy; Surface composition; Gallium;  
30 Indium; Surface chemical engineering

## 31 **1. Introduction**

32 X-ray Photoelectron Spectroscopy (XPS) on CIGS ( $\text{Cu}(\text{In,Ga})\text{Se}_2$ ) is an efficient method to provide  
33 surface chemical and quantitative information. The probed thickness is less than 10 nm when X-Ray  
34 excitation is provided by the Al-K $\alpha$  line. It is inside this thin external layer region that most of the  
35 crucial chemical engineering processes are conducted for all the CIGS based devices. So,  
36 determination of the CIGS surface chemistry is still a challenge which needs specific and reliable  
37 approaches as it will enable to efficiently orientate the surface chemistry and, so, to optimize  
38 properties at the CIGS front and back interfaces. This paper aims to contribute providing XPS  
39 characterizations of CIGS absorbers, starting from reference CIGS surface to certify the quantitative  
40 composition approach, to further extended on real practical cases. The CIGS surfaces have their  
41 proper chemical specificities, emphasized by the complexity of the surface parameters as poly-  
42 crystallinity, roughness, local surface steps, side chemical perturbations, differential grain boundaries  
43 reactivity and grains crystallographic orientations. Considering all these combined complex factors in  
44 addition to the quaternary character of the alloy, it is obvious that chemical composition  
45 determination must still be considered as a challenge to be taken up.

46 Our paper deals with this issue and is focused on a methodological approach enabling to determine  
47 as precisely as possible the GGI ratio: ( $[\text{Ga}]/([\text{Ga}]+[\text{In}])$ ) of CIGS absorber, main parameter, which  
48 governs the gap value [1-9]. Determining the exact GGI value is a central and difficult challenge for  
49 the cell conception. In particular, the surface absorber composition conditions the absorber/buffer  
50 layer interface energy diagram, then further cell efficiency issues. Considering the high surface  
51 sensitivity of XPS, this technique is a perfect nondestructive tool for the GGI determination of the  
52 outer part of the CIGS layer. To conduct a rigorous discussion, our metrological approach was first  
53 performed on reference CIGS surfaces presenting controlled surface chemistries. Reference surfaces  
54 can be obtained immediately after the layer growth, when it is possible, but also on a refreshed  
55 surface thanks to specific chemical treatments. In any case, for the present purpose, reference  
56 surfaces need to be oxides free, as well as free from binary selenide phases and all other side  
57 components, as sodium, commonly present on aged surfaces. Concerning CIGS, a “perfect-chemical”  
58 surface can be obtained by a combination of acidic [1], basic [10] and KCN aqueous treatments [10-  
59 14]. Possible combination [1] takes advantage of each treatment specificity to sequentially eliminate  
60 the surface oxides, the side binary selenide compounds and the elementary selenium. Nevertheless,  
61 the initial important roughness of CIGS surface is maintained. For a rigorous quantitative XPS  
62 approach, disposing of flattened surfaces up to few nanometers RMS (Root Mean Square) is also  
63 benefic to avoid relief artifacts (electrons backscattering...) and guarantee the homogeneity of the  
64 depth probed and the spatial origin of the photoelectrons.

65 In the present paper, a flattening step is then considered to help, at first, the fundamental  
66 quantitative approach by XPS analysis. It is obtained through a short time dipping in dilute aqueous  
67 acidic  $\text{Br}_2$  solution [15]. This etching step is completed by a final chemical cleaning to reach the  
68 targeted CIGS “reference” surface, oxide or selenide side phases free at the XPS detection limit. The  
69 access to the actual GGI value and not to an estimation is not so evident because, if compositional  
70 XPS data are easy to obtain, their transformation in actual composition of alloys is more complex due  
71 to the quantification procedure involving inherently a necessary correction of the photopeak area

72 (transmission, sensitivity factors values, escape depth model...) and other uncontrolled side  
73 perturbations among them the carbon surface contamination is of particular importance. Indeed,  
74 carbon surface contamination has to be considered as an attenuation factor of the photopeaks  
75 intensities measured. This attenuation varies with kinetic energies (KE) of the different main core  
76 levels used and distributed along the whole KE scale. So, adventitious carbon operates as a  
77 differential filter for photoelectrons with different KE. This induces possible differences between the  
78 XPS estimation obtained by different photopeaks combination employed for quantification and the  
79 reality of the alloy composition of the treated surface. In this paper we discuss the use of the Ga3d-  
80 In4d region, in narrow binding energy region. It can be consider as the better alternative to provide  
81 the closer value to the actual surface GGI determination. The interest of considering this specific  
82 energy window gathering Ga3d and In4d, in addition to the conventional Ga2p and In3d peaks, has  
83 been previously introduced by Bär et al. [16,17]. In the present work, we extend the argumentation  
84 to use the Ga3d-In4d spectral window to have a direct overview of GGI evolution. This narrow  
85 binding energy region allows working with equivalent escape depth and carbon attenuation levels. So  
86 a more accurate GGI determination is expected. To comfort the Ga3d-In4d window exploitation, a  
87 fitting procedure is developed on a reference surface of  $\text{In}_x\text{Ga}_{1-x}\text{As}$  desoxidized epilayer. For this III-V  
88 alloy, the GGI ratio value is ensured by a fine determination via other complementary  
89 characterization method. We show that the metallurgic composition of this reference alloy can  
90 therefore also be well determined by XPS. We discuss the extension of the fitting procedure to the  
91 practical case of the reference CIGS surface.

## 92 **2. Experiments**

### 93 **2.1. CIGS and InGaAs samples description and surfaces preparation by chemical** 94 **engineering**

95 The CIGS samples are supplied by ZSW (Zentrum für Sonnenenergie- und Wasserstoff-Forschung,  
96 Germany) [18].

97 CIGS is co-evaporated on Mo (600 nm) / glass (3 mm) substrates. The CIGS layers are provided with  
98 optimal GGI bulk ratio close to 0.30 and a thickness of 2.1  $\mu\text{m}$ . A large area sample was divided in  
99 equivalent area pieces (1x1 cm) to ensure the reliability of the comparative diagnostic. In the present  
100 case, the absence of usual Ga gradient in depth was verified through Secondary Ion Mass  
101 Spectrometry (SIMS) measurements, performed on an IMS7f CAMECA. Those results are not  
102 presented here.

103  $\text{In}_x\text{Ga}_{1-x}\text{As}$  epi-layer sample was grown by Metal Organic Vapors Phase Epitaxy process on InP (100).  
104 Sample thickness is nominally 160 nm which implies that the epitaxial layer is strained (no relaxation)  
105 on the InP substrate, then the Vegard Law can be used to determine by XRD (X-Ray Diffraction) the  
106 alloy composition. So the alloy composition of our reference layer has been derived from XRD  
107 rocking curve measurement and given as  $\text{In}_{0.517}\text{Ga}_{0.483}\text{As}$ .

108 The CIGS samples flattening is obtained thanks to an etching solution of HBr (0.20 mol L<sup>-1</sup>): Br<sub>2</sub> (0.02  
109 mol L<sup>-1</sup>): H<sub>2</sub>O (ultra-pure de-ionized water, 18.2 M $\Omega$ ) [15]. This etching process allowing a quasi layer  
110 by layer dissolution of the CIGS absorber is not selective and leaves the surface deoxidized and leads  
111 to a spectacular decrease of the surface roughness. More details can be found elsewhere [15, 19]. As  
112 Ga gradient is not present on the used samples (as confirmed by SIMS profiling measurements), the  
113 XPS responses do not depend on the immersion time. The etching time is fixed to obtain a smooth  
114 surface, still conformal and thick at the XPS scale. Samples are rinsed under ultra-pure de-ionized  
115 water (18.2 M $\Omega$ ) and dried with nitrogen flux. Then, as conventionally employed during the cell  
116 fabrication process, a wet chemical treatment based on a basic solution is performed using KCN (0.1  
117 mol L<sup>-1</sup>, 5 min) [10-14].  $\text{In}_x\text{Ga}_{1-x}\text{As}$  sample is deoxidized using an HCl solution (2 mol L<sup>-1</sup>, during 5 min).  
118 Finally, both CIGS and  $\text{In}_x\text{Ga}_{1-x}\text{As}$  samples are rinsed in ultra-pure water (18.2 M $\Omega$ ), dried under  
119 nitrogen and directly transferred into the XPS spectrometer.

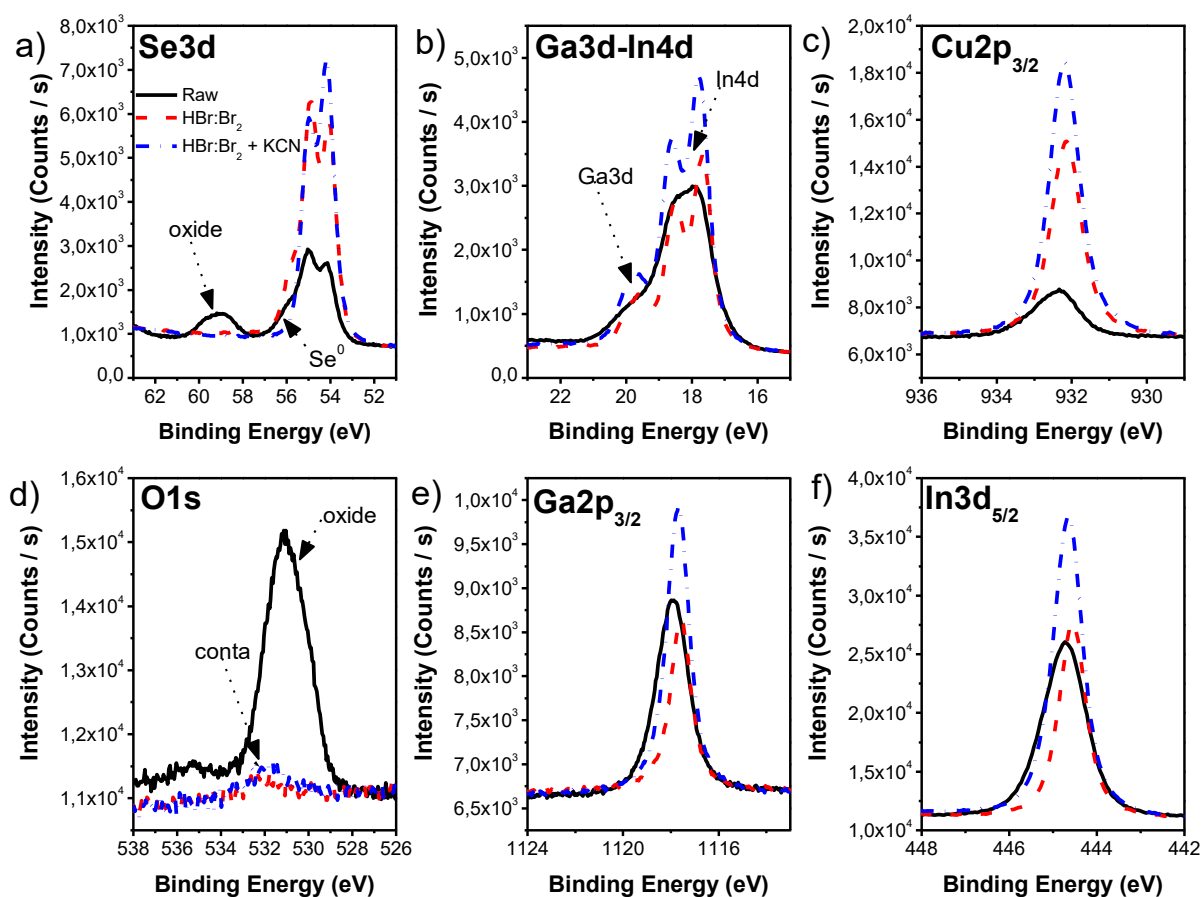
## 120        **2.2. X-ray Photoelectron Spectroscopy (XPS)**

121 XPS surface chemical analyses are carried out with a Thermo Electron K-Alpha<sup>+</sup> spectrometer using a  
122 monochromatic Al-K $\alpha$  X-Ray source (1486.6 eV). The X-Ray spot size is 400  $\mu$ m. The Thermo Electron  
123 procedure was used to calibrate the K-Alpha<sup>+</sup> spectrometer by using metallic Cu and Au samples  
124 intern references (Cu 2p<sub>3/2</sub> at 932.6 eV and Au 4f<sub>7/2</sub> at 84.0 eV). High energy resolution spectra are  
125 acquired using a Constant Analyser Energy mode 10 eV and 0.05 eV as energy step size. Data are  
126 processed using the Thermo Fisher scientific Avantage<sup>®</sup> data system. XPS spectra are treated using a  
127 Shirley background subtraction and XPS composition are deduced using the Sensitivity Factors, the  
128 transmission factor and inelastic mean-free paths from Avantage<sup>®</sup> library associated to the  
129 spectrometer. The fits are performed with Gaussian/Lorentzian mix.

## 130        **3. Results and Discussion**

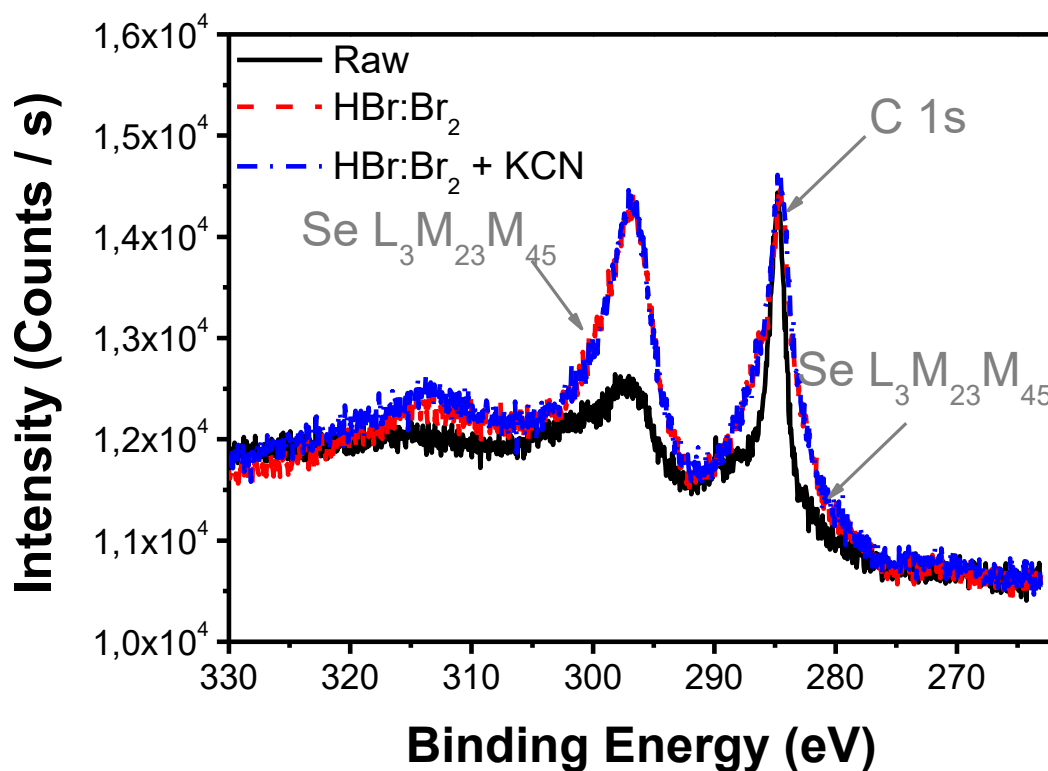
131 As previously shown, aqueous acidic bromide solutions [15] generate a constant etching rate process  
132 which progressively eliminates the initial roughness of the layers. Our final RMS roughness is always  
133 in the 5-10 nm range, compared to the 100-150 nm initial ones. However if the spectacular flattening  
134 is easily reachable, a question is the associated post etching surface chemistry. Figure 1 shows the  
135 XPS evolutions of the as-grown, of the HBr:Br<sub>2</sub>:H<sub>2</sub>O and then of the HBr:Br<sub>2</sub>:H<sub>2</sub>O and KCN treated  
136 surfaces. Modifications are observed for the Ga3d-In4d and Se3d regions, as well as for the regular  
137 core levels used in the literature Ga2p<sub>3/2</sub>, Cu2p<sub>3/2</sub> and In3d<sub>5/2</sub>. Starting from an initial oxidized CIGS  
138 surface [1], Br<sub>2</sub> etching [15] leaves CIGS surfaces without oxide layer but with low side Se<sup>0</sup> phase  
139 which amount depends strongly on the etching conditions. When it is presented, the Se<sup>0</sup> side phase  
140 on Se3d peak is evidenced by an additional feature with a shoulder contribution in the 56-57 eV  
141 range. This feature disappears after KCN treatment (Figure 1-a). The deoxidation efficiency is evident  
142 on the O1s signal, whose intensity is drastically decreased, after HBr:Br<sub>2</sub>:H<sub>2</sub>O etching (Figure 1-d).  
143 Moreover the Ga and In photopeaks present strongly thinned envelopes and the characteristic oxide  
144 contribution of the Se3d close to 59 eV disappears. All the photopeaks present higher intensities

145 after chemical treatments, in accordance with the decrease of the superficial carbon contamination  
 146 (Figure 2). A qualitative comparison between those intensities evolution show an expected Cu-  
 147 depletion on the as-grown [1]. Finally, the Cu signals  $\text{Cu}2p_{3/2}$  and Cu(LMM) Auger lines (not shown  
 148 here) of the chemically treated samples are characteristic of a Cu(I) contribution as expected for a  
 149 CIGS lattice. Note that in this case, the possible  $\text{Cu}_2\text{O}$  contribution which is difficult to discriminate  
 150 from Cu(I) in CIGS is easily eliminated due to the very low oxygen level and comforted because an  
 151 additional HCl dipping [1] does not change anything on copper signals.



152  
 153 *Figure 1: High energy resolution XPS spectra comparison of as-grown (solid black line) // etched with*  
 154 *HBr:Br<sub>2</sub> H<sub>2</sub>O solution (dash red line) // etched with HBr:Br<sub>2</sub>:H<sub>2</sub>O solution and KCN treated (dash-dot*  
 155 *blue line) CIGS surface: a) Se3d, b) Ga3d-In4d region, c) Cu2p<sub>3/2</sub>, d) O1s, e) Ga2p<sub>3/2</sub> and f) In3d<sub>5/2</sub>.*

156 The analysis of  $\text{Cu}2p_{3/2}$ ,  $\text{In}3d_{5/2}$ ,  $\text{Ga}2p_{3/2}$ ,  $\text{Se}3d$  and  $\text{O}1s$  photopeaks shows that after the final KCN  
157 treatment a very clean surface without selenide phase and detectable oxides is obtained. The oxygen  
158 signal intensity is very low and only related to adventitious carbon stacked to the surface during the  
159 sample manipulations. This suggests that  $\text{Ga}2p_{3/2}$ ,  $\text{In}3d_{5/2}$ ,  $\text{Cu}2p_{3/2}$  and  $\text{Se}3d$  energy distributions  
160 substantially narrowed, are representative of only one chemical environment: the CIGS one's. This  
161 diagnostic will be refined later in the text but this first examination of the photopeaks evolution  
162 demonstrates that a clean CIGS surface is obtained at the issue of the combined sequences. At first  
163 sight, the surface differs from a perfect reference only due to carbon sticking at the surface during  
164 the transfer. The adventitious carbon contamination is very difficult to evaluate due to  
165  $\text{Se}L_3M_{23}M_{45}/C1s$  overlapping (Figure 2) and will not be quantified here.



166

167 *Figure 2: C1s XPS spectra comparison as-grown (solid black line)// etched with HBr:Br<sub>2</sub> H<sub>2</sub>O solution*  
168 *(dash red line) // etched with HBr:Br<sub>2</sub>:H<sub>2</sub>O solution and KCN treated (dash-dot blue line) CIGS surface.*

169 Corrected XPS peaks intensities provide the XPS global chemical composition using the corresponding  
170 sensitivity factors (SF(Cu2p<sub>3/2</sub>): 18.147, SF(Ga2p<sub>3/2</sub>): 22.700, SF(In3d<sub>5/2</sub>): 19.112, SF(Se3d): 1.600 and  
171 SF (O1s): 2.881), the respective electron attenuation lengths and the transmission function of the  
172 analyzer. The resulting atomic percentages are presented in Table 1.

173

174 *Table 1: Atomic percentages of CIGS surfaces obtained from the Cu2p<sub>3/2</sub>, Ga2p<sub>3/2</sub>, In3d<sub>5/2</sub>, Se3d and*  
175 *O1s regions for different surface treatments; C1s contribution is not considered*

Atomic percentage (%)	Cu	Ga	In	Se	O
Raw surface	4.0	5.1	13.5	33.5	43.9
HBr:Br <sub>2</sub> surface	12.6	3.7	11.1	69.0	3.6
HBr:Br <sub>2</sub> + KCN surface	15.1	5.4	15.9	58.2	5.4

176

177 The direct calculation of the surface composition presented in Table 1 assumes that the layer is  
178 homogeneous within the matter probed by XPS. This is verified by XPS mapping. Moreover, the signal  
179 correction steps are complex, then the deduced XPS compositions must be used with a critical  
180 reasoning about a possible difference between the actual chemical composition and the XPS  
181 extracted one. Note that if we consider the C1s contribution, its intensity can be roughly estimated  
182 without a complete fitting procedure and give atomic percentage contribution for the carbon  
183 between 30-50% in a global composition, the corrected contribution for the other elements  
184 remaining in the same relative proportions.

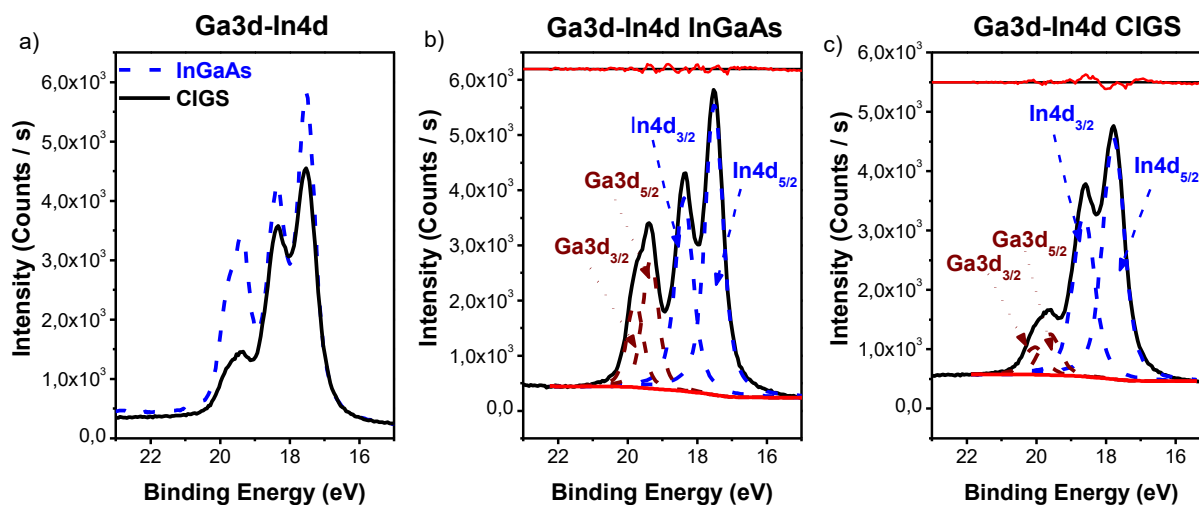
185 With our nearly “perfect-CIGS surface”, the GGI, obtained thanks to the Ga2p and In3d regions  
186 ( $GGI_{Ga2pIn3d}$ ), reaches the value of 0.25 ( $\pm 0.01$ ) (0.27 and 0.25 for raw and HBr:Br<sub>2</sub> surfaces ,  
187 respectively) when the expected value is 0.30. This probable under-estimation can be explained by  
188 the adventitious carbon over-layer acting, previously mentioned, as differential attenuation layer

189 depending on the KE of the photoelectrons. Concerning CIGS it is a key point because the foremost  
190 usual lines used are Ga2p<sub>3/2</sub> (KE: 370.6 eV), Cu2p<sub>3/2</sub> (KE: 555.6 eV), In3d<sub>5/2</sub> (KE: 1043.6 eV) and Se3d  
191 (KE: 1429.6 eV) whose photopeak kinetic energies are largely distributed over the 1486.6 eV range  
192 provided by the X-Ray Al anode. Then, corrections due to the carbon overlayer attenuation must be  
193 considered. Obviously, the differential attenuation is as a perturbation source for the apparent XPS  
194 composition and very difficult to deal with due to the fluctuation on the nature of the adventitious  
195 carbon contamination and complicated by its possible inhomogeneous sticking at the surface. As  
196 indicated above, the determination of the C content is not obvious requires to separate the C1s from  
197 Se(L<sub>3</sub>M<sub>23</sub>M<sub>45</sub>) lines (Figure 2) and, so, rarely considered. In addition, specific calibration to determine  
198 the differential attenuations is required. Another possibility consists in minimizing this effect by  
199 choosing a set of XPS peak with narrower distribution of KE, as previously proposed by Bär et al.  
200 [16,17].

201 CIGS's XPS response provides this opportunity through its Ga3d and In4d levels (Figure 1-b),  
202 appearing in the 30 eV to 10 eV spectral region. Then, we can work without differential signal  
203 balancing consideration. Moreover equal escape depths can be assumed for this set of lines and an  
204 absolute estimation of the GGI response of the material. Then, the only questionable parameters are  
205 the sensitivity factors ones. As the element III's distribution is grouped only over 6 eV range, the  
206 separation is sufficient between both to provide coherent fitting procedure when the CIGS surface is  
207 oxide free.

208 To ensure a reliable modeling procedure, so a fine determination of the reconstruction parameters is  
209 necessary, we choose to perform the Ga3d-In4d region reconstruction of a certified and deoxidized  
210 In<sub>x</sub>Ga<sub>1-x</sub>As/InP epilayer reference sample (In<sub>0.517</sub>Ga<sub>0.483</sub>As) Note that as expected, the relative energy  
211 position and intensities are totally reproducible on XPS mapping The comparison of the Ga3d-In4d  
212 region of the reference In<sub>x</sub>Ga<sub>1-x</sub>As/InP and CIGS layers is presented Figure 3-a. Both global shapes are  
213 similar, the main difference relying on the Ga and In contents in the two materials. The fitting

214 parameters have been compared to the one obtained on GaP and InP samples (same experimental  
215 conditions) for which only one fingerprint, either Ga or In, is visible.



216  
217 *Figure 3: High energy resolution XPS spectra comparison of CIGS (black solid line) and In<sub>x</sub>Ga<sub>1-x</sub>As (blue*  
218 *dash line) materials -a)- and simulations of b) In<sub>x</sub>Ga<sub>1-x</sub>As and c) CIGS Ga3d-In4d regions.*

219 Figure 3-b and Figure 3-c present the fitting simulations obtained for the Ga3d-In4d region for the  
220 In<sub>x</sub>Ga<sub>1-x</sub>As and CIGS layers. For both, the main constraints introduced in the simulation are related to  
221 the branching ratio (close to  $0.67 \pm 0.01$ ), as Ga3d and In4d present a d-level spin-orbit splitting, and  
222 to the FWHM (Full Width at Half Maximum) values, which are considered as equal for the 3/2 and  
223 5/2 d contributions. Concerning In4d, the spin-orbit splitting is perfectly established and obviously  
224 the same for both layers, as soon as a correct deoxidation has been performed. Its value is equal to  
225  $0.85 \pm 0.01$  eV. Regarding the spin-orbit splitting for Ga3d, it is less marked and needs very high  
226 resolution spectra to observe characteristic shape deformation. For the In<sub>x</sub>Ga<sub>1-x</sub>As layer, the spin-  
227 orbit splitting seems more resolved. So, using this support, the spin-orbit distance found for the Ga3d  
228 level is equal to  $0.44 \pm 0.02$  eV, in total agreement with our oxide free GaP samples ( $0.43 \pm 0.02$  eV).  
229 Using these fitting parameters, we obtain good simulation of the key Ga3d-In4d regions which has  
230 characteristic intensity ratios related to the atomic ratio between Ga and In present in In<sub>x</sub>Ga<sub>1-x</sub>As or  
231 CIGS layers. When the respective intensities are corrected from the atomic level sensitivity factors,

232 we access to the XPS  $G_{Ga3dIn4d}$  parameter. For our  $In_xGa_{1-x}As$  sample, a GGI equal to  $0.484 \pm 0.005$  is  
 233 determined using a factor sensitivity ratio (SF)  $SF_{Ga3d}/SF_{In4d}$  ( $1.412/3.601$ ) equal to 0.39 (THERMO@  
 234 Avantage Scientific data base). The XPS GGI deduced from the Ga3d-In4d region is then in perfect  
 235 agreement with the GGI (0.483) obtained by XRD, thereby validating the fitting parameters used.

236 The fitting parameters (branching ratio, spin-orbit splitting) obtained thanks to the reference sample  
 237 were then implemented to the Ga3d-In4d region of the CIGS sample (Figure 3-c) using the same  
 238 previous procedure. The  $G_{Ga3dIn4d}$  ratio is equal to  $0.29 (\pm 0.01)$ , which presents much more  
 239 coherence than the  $G_{Ga2pIn3d}$  ratio ( $0.25 \pm 0.01$ ) presented above. In addition, an interesting  
 240 difference is observed between the  $In_xGa_{1-x}As$  reference sample and the CIGS ones. Indeed, a  
 241 widening of the FWHM parameters for each element is noted to satisfactorily fit the CIGS Ga3d-In4d  
 242 region (Table 2). As information, FWHM for GaP and InP materials are also presented in Table 2,  
 243 which are equal to ones determine for  $In_xGa_{1-x}As$  sample.

244

245 *Table 2: FWHM parameters evolution for GaP, InP,  $In_xGa_{1-x}As$  and CIGS layers*

FWHM parameter (eV)	In4d <sub>5/2</sub>	In4d <sub>3/2</sub>	Ga3d <sub>5/2</sub>	Ga3d <sub>3/2</sub>
GaP	/	/	0.55	0.55
InP	0.63	0.63	/	/
$In_xGa_{1-x}As$	0.62	0.62	0.55	0.55
CIGS	0.74	0.74	0.71	0.71

246

247 To explain this widening on FWHM CIGS layer, several possibilities must be considered. As CIGS is a  
 248 polycrystalline material, a surface potential modulation could be considered, associated to the grain  
 249 boundaries distribution. Therefore, a slight modulation of the energy diagram can appear leading to

250 the widening of the FWHM photopeaks. Working with a CIGS monocrystal will remove this effect and  
251 provide a more accurate support for discussion.

## 252 **4. Conclusion**

253 With a combination of chemical treatments (acidic Br<sub>2</sub> etching followed by KCN dipping), a CIGS  
254 “reference” surface was obtained as support for GGI quantification obtained by XPS. From this  
255 reference surface, clean of residual oxides and side selenide phases, a determination of the GGI ratio,  
256 is then optimized. Comparing the  $GGI_{Ga3dIn4d}$  ( $0.29 \pm 0.01$ ) and the  $GGI_{Ga2p, In3d}$  ( $0.25 \pm 0.01$ ), we  
257 observe a slight but consequent difference. We attribute it to possible perturbations induced by the  
258 signals attenuation due to carbon contamination. Considering that the Ga3d-In4d region is restricted  
259 in an energy window of 10 eV, we assume that the attenuation effect is limited even nonexistent,  
260 suggesting that this window would be the most adapted to the quantification of GGI [16,17].  
261 However, this hypothesis needs correcting factors provided by library data bases to be accurate  
262 accurate, and particularly the sensitivity factors which, in this case, can be considered as the only one  
263 significant correction parameters. In order to comfort the validity of the sensitivity factors employed  
264 for the Ga3d-In4d region, we introduced, as reference sample, an III-V epitaxial layer  $In_xGa_{1-x}As$   
265 whose composition has been certified by XRD measurements. This epitaxial layer presents a similar  
266 Ga3d-In4d mixed window. On this reference sample, we determine the fitting parameters and we  
267 deduce a final XPS composition in total agreement with the expected one, validated by XRD  
268 measurements. So we consider that our correcting factors are validated. Therefore we apply these  
269 fitting parameters to the determination of the  $GGI_{Ga3dIn4d}$  on CIGS, which can now be considered as  
270 the actual GGI value at the surface. Moreover, we observe a slight widening of the XPS lines,  
271 interrogating on the small fluctuations of the potential at the surface. Finally, the lower GGI value  
272 obtained using regular core levels (Ga2p and In3d) can be consider as under-estimated, indicating  
273 that the perturbation of Ga2p intensity is more affected than the In3d’s one. This observation is  
274 coherent with the evolution of kinetic energies, as the Ga2p one is lowest than the In3d’s one,

275 leading to a Ga2p peak more affected by the attenuation layer than In3d's one. According to the  
276 carbon contamination level, the  $G_{Ga2p, In3d}$  determination can be underestimated, whereas the  
277  $G_{Ga3dIn4d}$  won't be affected. To reduce the carbon contamination, different chemical engineering  
278 treatments should be provided. Similarly, ionic Argon cluster bombardment can also be used. Both  
279 points will be extensively presented in a following paper. Furthermore, other key parameters such as  
280 CGI and Se balance can be studied using combinations in similar energy ranges [20].

## 281 **5. Acknowledgements**

282 Authors thank Wolfram Hempel from ZSW (Zentrum für Sonnenenergie- und Wasserstoff-Forschung,  
283 Germany) for CIGS samples supply.

284 Authors thank François Jomard (GEMAC, UVSQ) for SIMS measurements.

285 This work has been carried out in the framework of the project I of IPVF (Institut Photovoltaïque  
286 d'Ile-de-France). This project has been supported by the French Government in the frame of the  
287 program "Programme d'Investissement d'Avenir – ANR-IEED-002-01".

## 288 **6. References**

- 289 [1] A. Loubat, M. Bouttemy, S. Gaiaschi, D. Aureau, M. Frégnaux, D. Mercier, J. Vigneron, P. Chapon,  
290 A. Etcheberry, Chemical engineering of Cu(In,Ga)Se<sub>2</sub> surfaces: An absolute deoxidation studied  
291 by X-ray Photoelectron Spectroscopy (XPS) and Auger Electron Spectroscopy (X-AES) signatures,  
292 Thin Solid Films. 633 (2016) 87-91.
- 293 [2] K. Orgassa, U. Rau, H.W. Schock, I.U. Werner, Optical constants of Cu (In, Ga) Se<sub>2</sub> thin films from  
294 normal incidence transmittance and reflectance, in: Photovoltaic Energy Conversion, 2003.  
295 Proceedings of 3rd World Conference On, IEEE, 2003: pp. 372–375.
- 296 [3] S. Minoura, K. Kodera, T. Maekawa, K. Miyazki, S. Niki, H. Fujiwara, Dielectric function of  
297 Cu(In,Ga)Se<sub>2</sub>-based polycrystalline materials, Journal of Applied Physics. 113 (2013) 063505.

- 298 [4] S. Minoura, T. Maekawa, K. Kodera, A. Nakane, S. Niki, H. Fujiwara, Optical constants of Cu(In,  
299 Ga)Se<sub>2</sub> for arbitrary Cu and Ga compositions, *Journal of Applied Physics*. 117 (2015) 195703.
- 300 [5] S. Levchenko, L. Durán, G. Gurieva, M.I. Alonso, E. Arushanov, C.A. Durante Rincón, M. León,  
301 Optical constants of Cu(In<sub>1-x</sub>Ga<sub>x</sub>)<sub>5</sub>Se<sub>8</sub> crystals, *Journal of Applied Physics*. 107 (2010) 033502-  
302 033506.
- 303 [6] S. Levchenko, G. Gurieva, E.J. Friendrich, J. Trigo, J. Ramiro, J.M. Merino, E. Arushanov, M. Leon,  
304 Optical constants of CuIn<sub>1-x</sub>Ga<sub>x</sub>Se<sub>2</sub> films deposited by flash evaporation, *Mold. J. Phys. Sciences*. 9  
305 (2010) 148–155.
- 306 [7] M.I. Alonso, M. Garriga, C.A. Durante Rincón, E. Hernández, M. León, Optical functions of  
307 chalcopyrite CuGa<sub>x</sub>In<sub>1-x</sub>Se<sub>2</sub> alloys, *Applied Physics A: Materials Science & Processing*. 74 (2002)  
308 659–664.
- 309 [8] P.D. Paulson, R.W. Birkmire, W.N. Shafarman, Optical characterization of CuIn<sub>1-x</sub>Ga<sub>x</sub>Se<sub>2</sub> alloy thin  
310 films by spectroscopic ellipsometry, *Journal of Applied Physics*. 94 (2003) 879.
- 311 [9] M. Richter, C. Schubbert, P. Eraerds, I. Riedel, J. Keller, J. Parisi, T. Dalibor, A. Avellán-Hampe,  
312 Optical characterization and modeling of Cu(In,Ga)(Se,S)<sub>2</sub> solar cells with spectroscopic  
313 ellipsometry and coherent numerical simulation, *Thin Solid Films*. 535 (2013) 331–335.
- 314 [10] B. Canava, J. Vigneron, A. Etcheberry, D. Guimard, J.-F. Guillemoles, D. Lincot, S.O.S. Hamatly, Z.  
315 Djebbour, D. Mencaraglia, XPS and electrical studies of buried interfaces in Cu(In, Ga)Se<sub>2</sub> solar  
316 cells, *Thin Solid Films*. 403 (2002) 425–431.
- 317 [11] K. Ramanathan, F.S. Hasoon, S. Smith, D.L. Young, M.A. Contreras, P.K. Johnson, A.O. Pudov, J.R.  
318 Sites, Surface treatment of CuInGaSe<sub>2</sub> thin films and its effect on the photovoltaic properties of  
319 solar cells, *Journal of Physics and Chemistry of Solids*. 64 (2003) 1495–1498.
- 320 [12] J. Lehmann, S. Lehmann, I. Laueremann, T. Rissom, C.A. Kaufmann, M.C. Lux-Steiner, M. Bär, S.  
321 Sadewasser, Reliable wet-chemical cleaning of natively oxidized high-efficiency Cu(In,Ga)Se<sub>2</sub> thin-  
322 film solar cell absorbers, *Journal of Applied Physics*. 116 (2014) 233502.

- 323 [13] B. Canava, J. Vigneron, A. Etcheberry, J.F. Guillemoles, D. Lincot, High resolution XPS studies of Se  
324 chemistry of a Cu(In,Ga)Se<sub>2</sub> surface, Applied Surface Science. 202 (2002) 8–14.
- 325 [14] O. Roussel, M. Lamirand, N. Naghavi, J.F. Guillemoles, B. Canava, A. Etcheberry, Interfacial  
326 chemistry control in thin film solar cells based on electrodeposited CuIn(S,Se)<sub>2</sub>, Thin Solid Films.  
327 515 (2007) 6123–6126.
- 328 [15] M. Bouttemy, P. Tran-Van, I. Gerard, T. Hildebrandt, A. Causier, J.L. Pelouard, G. Dagher, Z. Jehl,  
329 N. Naghavi, G. Voorwinden, B. Dimmler, M. Powalla, J.F. Guillemoles, D. Lincot, A. Etcheberry,  
330 Thinning of CIGS solar cells: Part I: Chemical processing in acidic bromine solutions, Thin Solid  
331 Films. 519 (2011) 7207–7211.
- 332 [16] M. Bär, I. Repins, M. A. Contreras, L. Weinhardt, R. Noufi C. Heske, Chemical and electronic  
333 surface structure of 20%-efficient Cu(In,Ga)Se<sub>2</sub> thin film solar cell absorbers, Applied Physics  
334 Letters. 95 (2009) 052106-052109.
- 335 [17] E. Handick, P. Reinhard, R. G. Wilks, F. Pianezzi, T. Kunze, D.r Kreikemeyer-Lorenzo, L. Weinhardt,  
336 M. Blum, W. Yang, M. Gorgoi, E. Ikenaga, D. Gerlach, S. Ueda, Y. Yamashita, T. Chikyow, C. Heske,  
337 S. Buecheler, A. N. Tiwari, M. Bär, Formation of a K-In-Se Surface Species by NaF/KF  
338 Postdeposition Treatment of Cu(In,Ga)Se<sub>2</sub> Thin-Film Solar Cell Absorbers, Applied Materials &  
339 Interfaces. 9 (2017) 3581-3589.
- 340 [18] B. Dimmler, H.W. Schock, Scaling-up of CIS Technology for Thin-film Solar Modules, Progress in  
341 Photovoltaics: Research and Applications. 4 (1996) 425–433.
- 342 [19] A. Loubat, C. Eyfert, F. Mollica, M. Bouttemy, N. Naghavi, D. Lincot, A. Etcheberry, Optical  
343 properties of ultrathin CIGS films studied by spectroscopic ellipsometry assisted by chemical  
344 engineering, Applied Surface Science. 421 (2017) 643–650.
- 345 [20] M. Bär, J. Klaer, R. Félix, N. Barreau, L. Weinhardt, R. G. Wilks, Cl. Heske, H.-W. Schock, Surface  
346 Off-Stoichiometry of CuInS<sub>2</sub> Thin-Film Solar Cell Absorbers, IEEE Journal of Photovoltaics, 3,  
347 (2013), 828-832.

348

349 List of Figures and Captions

350 Figure 1: High energy resolution XPS spectra comparison of as-grown (solid black line)// etched with  
351 HBr:Br<sub>2</sub> H<sub>2</sub>O solution (dash red line) // etched with HBr:Br<sub>2</sub>:H<sub>2</sub>O solution and KCN treated (dash-dot  
352 blue line) CIGS surface: a) Se3d, b) Ga3d-In4d region, c) Cu2p<sub>3/2</sub>, d) O1s, e) Ga2p<sub>3/2</sub> and f)In3d<sub>5/2</sub>.

353 Figure 2: C1s XPS spectra comparison as-grown (solid black line)// etched with HBr:Br<sub>2</sub> H<sub>2</sub>O solution  
354 (dash red line) // etched with HBr:Br<sub>2</sub>:H<sub>2</sub>O solution and KCN treated (dash-dot blue line) CIGS surface.

355 Figure 3: High energy resolution XPS spectra comparison of CIGS (black) and InGaAs (blue) materials -  
356 a)- and simulations of b) InGaAs and c) CIGS Ga3d-In4d regions.

357 Table 1: Atomic percentages of CIGS surfaces obtained from the Cu2p<sub>3/2</sub>, Ga2p<sub>3/2</sub>, In3d<sub>5/2</sub>, Se3d and  
358 O1s regions for different surface treatments; C1s contribution is not considered

359 Table 2: FWHM parameters evolution for GaP, InP, In<sub>x</sub>Ga<sub>1-x</sub>As and CIGS layers